Available online at www.sciencedirect.com
SCIENCE DIRECT®
Journal of Sound and Vibration 262 (2003) 291–307
JOURNAL OF SOUND AND VIBRATION
www.elsevier.com/locate/jsvi

Damping identification using a continuous wavelet transform: application to real data

J. Slavič, I. Simonovski, M. Boltežar*

Faculty of Mechanical Engineering, University of Ljubljana, Aškerčeva 6, 1000 Ljubljana, Slovenia

Received 29 October 2001; accepted 12 February 2002

Abstract

A continuous wavelet transform (CWT) based on the Gabor wavelet function is used to identify the damping of a multi-degree-of-freedom system. The common procedures are already known, especially the identification with a Morlet CWT. This study gives special attention to the following: a description of the instantaneous noise, the edge-effect of the CWT, the frequency-shift of the CWT, the bandwidth of the wavelet function and the selection of the parameter σ of the Gabor wavelet function of the CWT. The procedures are demonstrated using several numerical examples and on signals acquired from the lateral vibration of a uniform beam. The study demonstrates the advantages of using the amplitude and phase methods, both of which provide information about the instantaneous noise. The procedures presented are appropriate for automating the identification process.

1. Introduction

The damping of dynamic systems is the dissipation of vibration energy. Usually, a considerable amount of this energy dissipates inside the system, mostly in the form of heat, while the rest dissipates outside the system in the form of acoustic radiation, transmission to other dynamic systems, etc.

Compared to an estimation of the stiffness and mass properties of multi-degree-of-freedom (MDOF) systems an estimation of the damping parameters is more difficult. The factors affecting damping mechanisms include friction on the atomic/molecular level, dry friction, viscous friction in fluids, etc., and so it is often difficult to describe in detail the real physical background using mathematical means. As a consequence of this, a number of simplified models were developed. Of

*Corresponding author. Tel.: + 386-1-4771-608 fax: + 386-1-2518-567.
E-mail address: miha.boltezar@fs.uni-lj.si (M. Boltežar).

0022-460X/03/$ - see front matter
PII: S0022-460X(02)01032-5

these models, the model of *viscous damping* is the most widely used, it assumes that the damping force is proportional to the velocity of oscillation; and so it follows that the work done by one oscillation cycle depends on the frequency of oscillation. Another commonly used model is the model of *structural damping*, where the work done in one cycle is independent of the oscillation frequency and where the dissipation of vibrational energy is proportional to the square of the amplitude [1]. To overcome the shortcomings of the different models the model of equivalent viscous damping is used. In this paper the damping is discussed in terms of the damping ratio, i.e., the fraction of critical damping. As a result, the damping matrix can be assumed to be proportional to the mass or stiffness matrix, so the system of differential equations can be uncoupled [1].

A number of damping measures and criteria are used to characterize structural damping [1–3]. An overview of several time, frequency and time–frequency domain techniques can be found in Staszewski [4]. In his work, Staszewski introduced a method for estimating the damping ratio based on the continuous wavelet transform (CWT) and the Morlet wavelet function. Besides being useful in several other applications [5–7], this time-scale method appears to be appropriate for estimating the damping in MDOF systems [4,8–13].

Argoul et al. [8] proposed a new, weighted integral transform. They showed that the co-ordinates of the extreme of the imaginary part of the new integral transform provide a good estimation of the modal frequencies and the damping ratios. Yin and Argoul [9] used a slightly different integral transform: with an additional parameter they were able to identify the modal parameters of linear systems, even with strong coupled modes. In contrast, Lamarque et al. [10] and Hans et al. [11] used a wavelet-based formula which is similar to the logarithmic decrement formula. This method simultaneously provides the modal decoupling and an estimate of the damping ratio.

The present work is closely related to the Staszewski [4] method, which is based on a wavelet reconstruction formula for asymptotic signals. In this paper some extensions of the method will be presented.

For the sake of completeness, Section 2 gives the background to the CWT and the basic concept of damping identification using the CWT. Section 2 also discusses some extensions of the Staszewski method: the identification of damping using the Gabor wavelet and the quantitative characterization of close modes. Further extensions of the Staszewski method are given in Sections 3 and 4. Section 3 discusses the edge-effect of the CWT and Section 4 the instantaneous signal-to-noise ratio (SNR) and the instantaneous normalized mean square error (nMSE). Sections 5 and 6 provide applications to real data, with Section 6 paying special attention to the experimental data of a uniform beam.

2. Estimation technique

2.1. Theoretical background of the wavelet transform

In this subsection only a few basic definitions are presented; for an exhaustive study the reader should refer to other literature, e.g., Refs. [14,15].

The CWT of the signal $x(t) \in L^2(\mathbf{R})$ is defined as

$$Wx(u,s) = \int_{-\infty}^{+\infty} x(t)\psi^*_{u,s}(t)\,\mathrm{d}t, \tag{1}$$

where u and s are the translation and scale/dilation parameters, respectively [16], and $\psi^*(t)$ is the complex conjugate of the basic wavelet function $\psi(t) \in L^2(\mathbf{R})$.

The wavelet function is a normalized function (i.e., the norm is equal to 1) with an average value of zero:

$$\|\psi(t)\|^2 = \int_{-\infty}^{+\infty} |\psi(t)|\,\mathrm{d}t = 1, \tag{2}$$

$$\bar{\psi}(t) = \int_{-\infty}^{+\infty} \psi(t)\,\mathrm{d}t = 0. \tag{3}$$

Table 1 shows the norm and the mean values of the Morlet and Gabor wavelet functions [5]. In both cases the selection of suitable parameters σ and η makes the mean value very close to zero. While the norm of the Gabor wavelet is equal to 1, the norm of the Morlet wavelet is not. However, the Morlet wavelet function can be normalized by multiplying it by $1/\sqrt[4]{\pi}$. The normalized Morlet wavelet function is identical to the Gabor wavelet function with the parameter $\sigma = 1$. The additional parameter σ of the Gabor wavelet function provides the possibility of adapting the time and frequency spread and will be discussed later in this paper.

The translated and dilated wavelet function is defined as

$$\psi_{u,s}(t) = \frac{1}{\sqrt{s}}\psi\left(\frac{t-u}{s}\right). \tag{4}$$

The Gabor wavelet function is defined as

$$\psi_{Gabor}(t) = \underbrace{\frac{1}{(\sigma^2\pi)^{1/4}}\mathrm{e}^{-t^2/(2\sigma^2)}}_{Gaussian\ \ window} \cdot \mathrm{e}^{\mathrm{i}\eta t}, \tag{5}$$

where parameter σ and the initial scale define the time and frequency spread of the Gabor wavelet function [7]; η is the parameter of frequency modulation.

In this study the term "normalized parameter σ" ($\sigma_{1\ \mathrm{Hz}}$) is used; this is the σ that would be used in the case of a signal with a frequency of 1 Hz. The appropriate parameter σ for any other frequency is: $\sigma_{1\ \mathrm{Hz}}\Delta t$, where Δt is the time step of the discretization.

Table 1
The norm and the mean value of the Morlet and Gabor wavelets

Property	Gabor	Morlet
$\|\psi(t)\|^2$	1	π
$\bar{\psi}(t)$	$\sqrt[4]{4\,\pi\sigma^2}\,\mathrm{e}^{-\eta^2\,\sigma^2/2}$	$\mathrm{e}^{-\eta^2}\,\sqrt{2\,\pi}/2$

The relation between the instantaneous scale s and the instantaneous angular velocity ω of the Gabor wavelet function is defined as

$$\omega(s) = \frac{\eta}{s}. \tag{6}$$

A very useful property of the CWT is its linearity:

$$\left(W \sum_{i=1}^{N} \alpha_i \; x_i \right)(u,s) = \alpha_i \sum_{i=1}^{N} (W \; x_i)(u,s), \tag{7}$$

which makes it possible to analyze each ith component x_i of a multi-component signal $\sum_{i=1}^{N} \alpha_i x_i$, where α_i is a constant.

2.2. Damping identification using a wavelet transform

It is assumed that the signal $x(t)$ is sinusoidal (8) and asymptotic, i.e., the signal's amplitude varies slowly compared to the variation of its phase [17]

$$x(t) = A(t) \cos \varphi(t). \tag{8}$$

In the case of such a signal its CWT can be approximated by a simple function. Staszewski [4] and Ruzzene et al. [18] used the Morlet wavelet function, and as a consequence they used the CWT approximation as defined by Delprat et al. [19]. In this paper the approximation of the CWT based on the Gabor wavelet function is used (for the derivation see Appendix A):

$$Wx(u,s) = \tfrac{1}{2} A(u) \hat{\psi}_{Gabor_{u,s}}(\varphi'(u), \sigma, \eta) \, \mathrm{e}^{\mathrm{i} \, \varphi(u)} + Er\big(A'(t), \varphi''(u)\big), \tag{9}$$

where the Fourier transform of the translated and scaled Gabor wavelet function is defined as

$$\hat{\psi}_{Gabor_{u,s}}(\omega, \sigma, \eta) = (4\pi\sigma^2 s^2)^{1/4} \, \mathrm{e}^{-(\omega - \eta/s)^2 \sigma^2 s^2/2} \, \mathrm{e}^{-\mathrm{i}\,\omega\,u}. \tag{10}$$

The approximation error $Er(A'(t), \varphi''(u))$ can be neglected if the derivative of the phase is greater than the bandwidth $\Delta\omega$ [14]:

$$\varphi'(u) \geqslant \Delta\omega. \tag{11}$$

The bandwidth $\Delta\omega$ of the translated and scaled Gabor wavelet function is defined as [14]

$$e^{z_1} = \frac{|\hat{w}_{Gauss}(s\,\omega, \sigma)|}{|\hat{w}_{Gauss}(0, \sigma)|} \ll 1 \quad \text{where } |s\,\omega| \geqslant \Delta\omega, \tag{12}$$

where $\hat{w}_{Gauss}$ is the Gaussian window (see Eq. (5)).

It follows that the bandwidth of the wavelet transform is

$$\Delta\omega(s) = \sqrt{\frac{-2\,z_1}{\sigma^2 s^2}}, \tag{13}$$

where the parameter z_1 needs to be chosen; if $z_1 = -8$ (the value used in this study) is chosen then the value of the wavelet at the bandwidth is only $34 \times 10^{-3}\%$ of the maximum value.

For the CWT of any two components i and j of a multi-component signal not to interfere, the maximum of the bandwidth $\Delta\omega(s_i)$ and $\Delta\omega(s_j)$ should be smaller than the frequency difference of i

and j [14]:

$$(\varphi_i'(u) - \varphi_j'(u)) \geqslant \max\{\Delta\omega(s_i), \Delta\omega(s_j)\}. \tag{14}$$

The time-scale representation of the energy concentration of the CWT is called the *ridge*. Ridges are described with the use of curves $s = s(u)$. In other words, ridges represent the frequency content of the analyzing signal with a high density of energy, which is dependent on the time (translation u). The values of the CWT that are restricted to the ridge are called the *skeleton* of the CWT–$Wx(u, s(u))$.

In the following the free response of a damped signal is focussed upon [1]:

$$x(t) = A_0 e^{-\zeta\omega_0 t} \cos(\omega_0 \sqrt{(1-\zeta^2)}\, t + \phi). \tag{15}$$

With the CWT it is possible to determine only the damped angular velocity $\omega_d = \omega_0\sqrt{1-\zeta^2}$, which differs slightly from the undamped natural angular velocity ω_0. In future derivations ω_d must be used instead of ω_0; however, because the damping ratio ζ is usually small ($\zeta \ll 1$) the error is insignificant. In dynamics this substitution is usual.

The procedure for damping-ratio extraction is now just the same as in the case of the Morlet wavelet [4]. First, Eq. (10) is inserted into Eq. (9) and the error part is neglected. Because attention was paid to the ridge, the angular velocity of the Gabor wavelet function ($\omega = \eta/s$) is equal to the angular velocity of the signal (ω_d), and as a consequence the term $e^{-(\omega_d - \eta/s)^2 \sigma^2 s_0^2/2}$ is equal to 1.

Finally, the next expression is derived

$$\ln\left(\frac{2|Wx(u, s(u))|}{(4\pi\,\sigma^2 s(u)^2)^{1/4}}\right) \approx -\zeta\omega_d\, u + \ln A_0. \tag{16}$$

It is clear that this equation represents a linear function and from its slope the damping ratio ζ can be estimated.

To reconstruct the signal the following functions can be derived:

$$\varphi(u) = \arctan\frac{\mathrm{Im}(Wx(u, s(u)))}{\mathrm{Re}(Wx(u, s(u)))}, \tag{17}$$

$$A(u) \approx \frac{2|Wx(u, s(u))|}{(4\pi\,\sigma^2 s(u)^2)^{1/4}}. \tag{18}$$

Now the only problem is the characterization of the ridge $s(u)$.

2.3. Ridge detection

Detailed explanations of the various methods for ridge extraction can be found elsewhere [4,17–20]. For the sake of completeness a brief explanation of the three simplest methods is given here. The first method is called the cross-section method (CM). It is based on the pre-known damped frequency ω_d. The ridge is constant and is defined as

$$s(u) = \frac{\eta}{\omega_d}. \tag{19}$$

The amplitude method (AM) is based on the maxima of the CWT, while the phase method (PM) is based on matching the angular velocity of the CWT with the angular velocity of the wavelet

function. It is known that the natural frequencies of linear systems have a constant angular velocity, so extreme searching for the instantaneous frequency seems needless, but the point lies elsewhere. The search algorithms return information about the instantaneous noise; when the level of noise is too high the detected instantaneous natural frequency will deviate from the expected natural frequency. By defining the maximum deviation range the return information can be used to interrupt the identification procedure of damping.

3. The edge-effect

Fig. 1 shows the difference between the CWT of an infinite sinusoidal signal with constant amplitude (a) and the CWT of a finite signal $x(t) \neq 0$, if $\{0.0 \leqslant t \leqslant 0.5\}$ in part (b) of the figure.

The difference arises because of the nature of the CWT. According to Eq. (1) the frequency spectrum at some translation u is calculated with the help of a wavelet in the neighbourhood of u. At the beginning and at the end of the signal a part of the wavelet is outside the signal (Fig. 2). The CWT at the edges of the signal is therefore not proportional to the CWT when the window is almost entirely in the signal; this is called the *edge-effect*. There is no known method to eliminate this problem, so this study focused on characterizing the time when the edge-effect is not negligible.

For the case of a Gaussian window the time-width (u_{wd}) of the edge-effect is

$$e^{z_2} = \frac{w_{Gauss_{u,s}}(t = -u_{wd}, \sigma)}{w_{Gauss_{u,s}}(t = 0s, \sigma)}, \tag{20}$$

which leads to

$$u_{wd} = \pm s\,\sigma\sqrt{-\tfrac{2}{3}z_2}. \tag{21}$$

The parameter z_2 needs to be chosen. If the damping ratio is expected to be very small then the edge-effect is more noticeable and the parameter z_2 should be more carefully chosen. For example, in practice $z_2 = -20$ is needed for a damping ratio of $\zeta \approx 100 \times 10^{-6}$ and $z_2 = -10$ is enough for a damping ratio of $\zeta \approx 100 \times 10^{-3}$.

The parameter σ of the Gabor wavelet is the only parameter that can be changed significantly. If a smaller value for σ is chosen, the edge-effect is less noticeable; but the consequence of this is a larger frequency spread of the wavelet function, this means that the frequency bandwidth gets

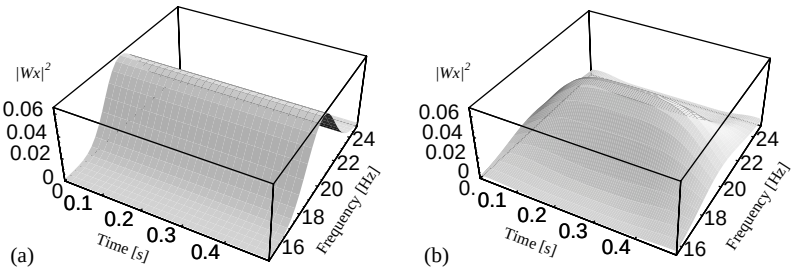

Fig. 1. Wavelet transform of a infinite signal (a) and a finite signal (b).

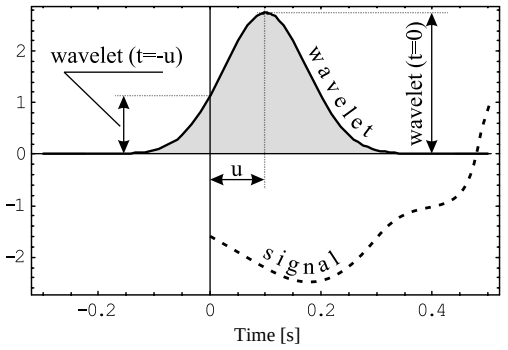

Fig. 2. Edge-effect in the time domain.

larger and close modes are more difficult to extract. On the other hand, a larger value of σ is more appropriate for analyzing close modes, but the consequence is not only a larger edge-effect but also the danger of losing the time locality of the wavelet transform.

However, usually we can afford a small σ parameter, but then we come to the next problem—the frequency-shift of the CWT amplitude extreme.

4. Frequency-shift of the CWT amplitude extreme

An obvious frequency-shift of the amplitude extreme of the CWT occurs in the case of a small parameter σ. The size of this shift can be defined analytically.

If there is a sinusoidal signal $x(t) = A_0 \cos \omega_0 t$ of constant amplitude A_0 and of constant angular velocity ω_0, then its CWT can be derived exactly:

$$Wx(u,s) = \int_{-\infty}^{+\infty} A_0 \cos(\omega_o t)\, \psi^*_{Gabor_{u,s}}(t)\, \mathrm{d}t, \tag{22}$$

$$Wx(u,s) = \frac{A_0}{2}(4\pi s^2 \sigma^2)^{1/4} \mathrm{e}^{-\mathrm{i}\, u\, \omega_0 - \sigma^2(\eta + s\, \omega_0)^2/2}(1 + \mathrm{e}^{2\,\mathrm{i}\, u\, \omega_0 + 2s\, \eta\, \sigma^2\, \omega_0}). \tag{23}$$

To find the extreme of this CWT the first derivative at s is sought. To simplify the task the part $\sqrt{s}\,\mathrm{e}^{-\sigma^2(\eta+s\,\omega_0)^2/2} \approx 0$ is neglected. It is found that the extreme is

$$s = \frac{\eta\,\sigma + \sqrt{2 + \eta^2\,\sigma^2}}{2\,\sigma\,\omega_0}. \tag{24}$$

With the use of the second derivative it can be verified that the extreme is a maxima in the neighbourhood of $s = \eta/\omega_0$.

According to Eq. (6) the frequency-shift is

$$\omega - \omega_0 = \left(\frac{\eta}{s}\right) - \left(\frac{\eta\,\sigma + \sqrt{2 + \eta^2\,\sigma^2}}{2\,\sigma\,s}\right) = \left(\frac{\eta - \sqrt{2/\sigma^2 + \eta^2}}{2\,s}\right). \tag{25}$$

Fig. 3 shows the ridges of the CWT defined on the amplitude maxima of the wavelet transform based on the Gabor wavelet function of a 311.3 Hz signal; part (a) shows the ridge that takes no

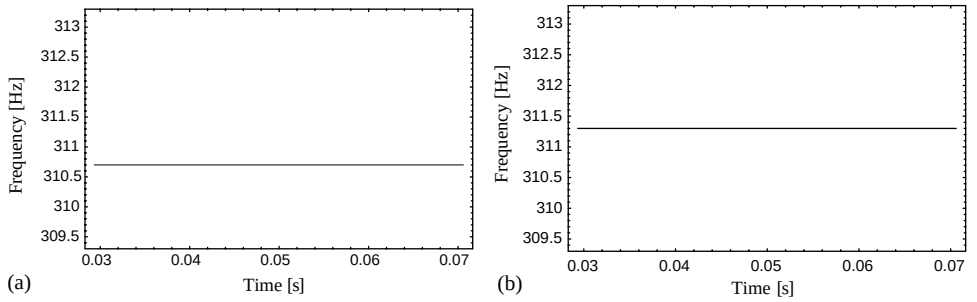

Fig. 3. (a) The ridge of the CWT defined on the amplitude extreme; (b) Same as (a) but taking into account the frequency-shift.

account of the frequency-shift, while part (b) shows the ridge when the frequency-shift is taken into account.

5. Instantaneous SNR and nMSE

5.1. Instantaneous SNR

In the case of a transient signal the classical definition of the SNR (Eq. (26)) is inappropriate. Fig. 4a shows a signal with zero mean Gaussian noise $SNR = 30\,\mathrm{dB}$:

$$SNR = 10 \log_{10}\left(\frac{\mathrm{var}(signal)}{\mathrm{var}(noise)}\right). \tag{26}$$

However, if it is assumed that the variance of the noise is constant (or nearly constant), then it is possible to calculate the instantaneous SNR ratio. It is clear that the mean value of a sinusoidal signal with a constant amplitude A_0 is equal to zero:

$$\mathrm{mean}(A \sin \omega t) = \lim_{T \to \infty} \frac{1}{2T} \int_{-T}^{+T} A \sin \omega t \, \mathrm{d}t = 0. \tag{27}$$

The variance of the same signal is

$$\mathrm{var}(A \sin \omega t) = \lim_{T \to \infty} \frac{1}{2T} \int_{-T}^{+T} (\mathrm{mean}(A \sin \omega t) - A \sin \omega t)^2 \, \mathrm{d}t, \tag{28}$$

$$\mathrm{var}(A \sin \omega t) = \frac{A^2}{2}. \tag{29}$$

Consequently, the instantaneous variance of the free damped response (15) is

$$\mathrm{var}(x(t)) = \frac{A_0^2 \, \mathrm{e}^{-2\,\zeta\omega_d\, t}}{2}. \tag{30}$$

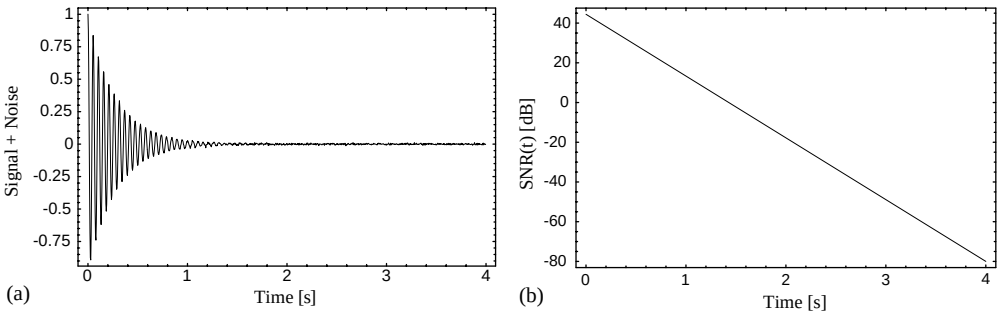

Fig. 4. (a) The signal of $SNR = 30\,\mathrm{dB}$; (b) the instantaneous SNR.

And finally, the instantaneous SNR is

$$SNR(t) = 10\log_{10}\left(\frac{A_0^2\,\mathrm{e}^{-2\,\zeta\omega_d\,t}}{2\,\mathrm{var}(noise)}\right). \tag{31}$$

Fig. 4b shows the instantaneous SNR of the signal with an average $SNR = 30\,\mathrm{dB}$ shown in Fig. 4a. The difference between the average SNR, which is 30 dB, and the instantaneous SNR, which ranges from 44 to $-80\,\mathrm{dB}$ can be seen.

While a signal is analyzed at nearly constant frequency it must be borne in mind that the power of noise is frequency dependent. Often colours are used to describe noise: purple, blue, white, pink and red/brown. Usually, the most important are white noise, which is independent of frequency, and pink noise, the power of which is proportional to $1/f$. Later in the paper the allowed frequency deflection will be introduced. If this deflection is set too wide then maybe the assumption of constant frequency does not hold and it might be expected that the actual noise ratio will be slightly higher or lower than that calculated on the assumption of a constant variance of noise.

5.2. Instantaneous nMSE

The nMSE of two signals is defined as [21]

$$nMSE(x,y) = \frac{1}{N\,\mathrm{var}(x)}\sum_{k=1}^{N}(x_k - y_k)^2, \tag{32}$$

where x is the theoretical impulse response function, y is the recovered response function, and N is the discrete length of functions x and y.

To calculate the instantaneous nMSE a rectangular window was used, the width of the window being $\pm 2\sigma s(u)$. The width was chosen according to the width of the Gaussian window used in the CWT at 95% of the area [22].

The instantaneous nMSE used in this study is defined as

$$nMSE(x,y)(u) = \frac{1}{N\,\mathrm{var}(x)}\sum_{k=1}^{N} w_k(u)\,(x_k - y_k)^2, \tag{33}$$

where $w_k(u)$ represents the rectangular window

$$w_k(u) = \begin{cases} 1, & |u - t_k| \leqslant 2\sigma s(u), \\ 0, & \text{otherwise.} \end{cases} \tag{34}$$

A similar procedure could also be used in the case of the instantaneous SNR.

6. Numerical example

In this Section numerical examples are given. The basic intention is to make some additional statements that refer to practical examples.

6.1. Resistance to noise

In this subsection only the signals of single-degree-of-freedom systems are used; the reason for this is that the instantaneous SNR can only be calculated exactly for such a signal. The parameters of three sample signals are given in Table 2. The first signal is a low-frequency signal with high damping, the second is a high-frequency signal of 647 Hz and the last is also a high-frequency signal but with small damping. The frequency resolution of the CWT was chosen to be approximately 0.05% of the signal frequency. The normalized parameter σ (the σ for the 1 Hz signal) of the Gabor wavelet function was chosen according to Fig. 5a.

The identification data is given in Table 3. The allowed frequency deviation was set to .5% of the signal frequency.

Special attention is to be given to signal 1 (Fig. 4a). Fig. 4b shows the instantaneous SNR of signal 1. The time-window of the CM is the whole time of the signal without the time-width on both ends. The logarithm of the amplitude is shown in Fig. 5b (see also Eq. (16)). It is clear that

Table 2
Parameters of discrete signals and their CWT

Parameter	Signal 1	Signal 2	Signal 3	Note
Discrete signals				
A_0	1.0	1.0	1.0	Amplitude
f (Hz)	19	647	2003	Frequency of signal
ζ	0.0300	0.0020	0.0001	Damping ratio
T (s)	4	1	1	Time-length
N	1000	6500	20000	Number of discrete points
SNR (dB)		30		Average SNR
Wavelet transform				
$\sigma_{1\,\mathrm{Hz}}$	2	4	7	Normalized σ
σ	0.0080	0.00062	0.00035	Parameter σ
Δf (Hz)	0.015	0.3	1	Frequency resolution
η (Hz)	250	6500	20000	Frequency modulation
u_{wd} (s)	0.272	0.016	0.009	Time-width

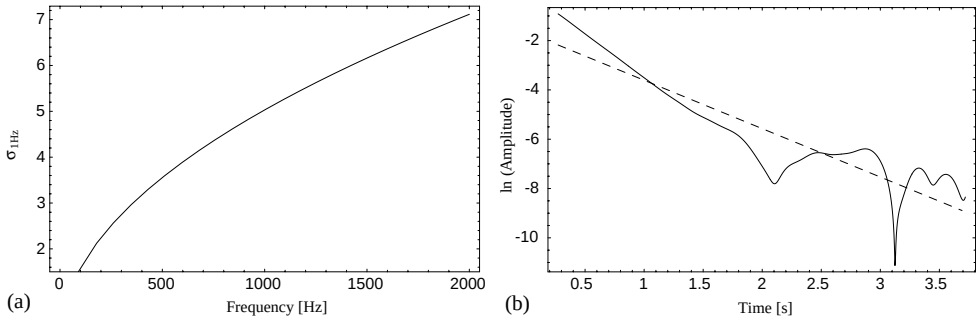

Fig. 5. (a) The normalized parameter σ; (b) logarithm of the amplitude of the signal 1, —signal, - - - linear regression.

Table 3
Damping identification.

Method	SNR (dB)	Time-window (s)	ζ	Er$_\zeta$ (%)
Signal 1 (ζ_{teor} = 30e-3)				
CM	36 to −71.3	0.272–3.720	16.4e–3	−45.20
AM	36 to 5.12	0.272–1.264	29.8e–3	−0.84
PM	36 to 5.00	0.272–1.268	29.7e–3	−0.86
Signal 2 (ζ_{teor} = 2e–3)				
CM	41 to −27.4	0.016–0.9844	1.9e–3	−3.02
AM	41 to 1.57	0.016–0.5739	2.0e–3	0.96
PM	41 to 1.60	0.016–0.5735	2.0e–3	0.96
Signal 3 (ζ_{teor} = 500e–6)				
CM	40.5 to −13.20	0.009–0.9909	499.6e–6	−0.09
AM	40.5 to −8.42	0.009–0.9041	498.3e–6	−0.34
PM	40.5 to −8.44	0.009–0.9044	498.3e–6	−0.33

the linear regression is not a suitable approximation. The maximum SNR is 71.3 dB. The damping ratio estimation is, as expected, poor. On the other hand, the AM and PM give better results. The ridge of the PM is shown in Fig. 6a, according to Table 3 and Fig. 4b the $SNR(t)$ at the break point is 5 dB. This break point occurs when the ridge frequency deviates from the expected frequency by more than $\pm 0.5\%$. The nMSE at the time of break is negligible, but this would rapidly grow after about −5 dB of SNR (Fig. 6b). The identification using the AM does not differ significantly from the one using PM.

From Table 3 it can be seen that the identification of the damping ratio of signals 2 and 3 is also very good. Note that the defined deviation of $\pm 0.5\%$ could be greater in the case of a low-frequency signal and smaller in the case of a high-frequency signal. However, if the length of the signal permits the identification of the low-noise part of the signal, then the deviation should be smaller.

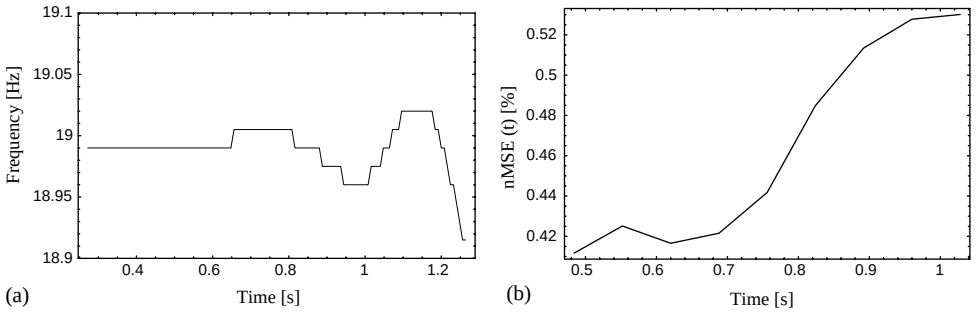

Fig. 6. Ridge of signal 1 by PM; (b) normalized MSE(t) for the case of the PM.

Table 4
Parameters of discrete signal 4 and its CWT

Parameter	Component 1	Component 2	Note
Discrete signal			
A_0	1.0	1.0	Amplitude
f [Hz]	19	23	Frequency of signal
ζ	0.030	0.015	Damping ratio
T [s]	4	4	Time length
N	1000	1000	Number of discrete points
SNR [dB]	30	30	Average SNR
Wavelet transform			
$\sigma_{1\,\mathrm{Hz}}$	3	3	Normalized σ
σ	0.012	0.012	Parameter σ
Δf (Hz)	0.015	0.015	Frequency resolution
η (Hz)	250	250	Frequency modulation
u_{wd} (s)	0.408	0.337	Time-width
$\Delta\omega$ (Hz)	4.03	4.88	Bandwidth

6.2. The identification of damping at close modes

In the case of a signal with several natural frequencies the condition of Eq. (14) needs to be considered. Here a signal of two natural frequencies is analyzed, although the procedure for more natural frequencies is similar. The parameters of signal 4 are given in Table 4.

Compared to signal 1 the parameter σ of the Gabor wavelet is higher ($\sigma_{1\,\mathrm{Hz}} = 3$); the frequency spread is therefore more localized. Actually, the bandwidths are 4 and 4.9 Hz (in the case of $\sigma_{1\,\mathrm{Hz}} = 2$, the bandwidths are 6 and 7.3 Hz). Because the frequency difference of both components is 4 Hz, the second component influences the CWT of the first component; but the influence of the first component on the second one is negligible. Larger error in the damping identification of the first component is therefore actually expected (Table 5). The instantaneous SNR given in the table is calculated for a one-component signal of each frequency and therefore mentioned for orientation only.

Table 5
Damping identification

Method	SNR (dB)	Time-window (s)	ζ	Er$_\zeta$ (%)
Signal 4–component 1 ($\zeta_{teor} = 30$e-3)				
CM	31.7 to −67.1	0.408–3.584	15.06e-3	−49.80
AM	31.7 to −15.2	0.408–1.916	27.8e-3	−7.46
PM	31.7 to −14.8	0.408–1.904	27.8e-3	−7.21
Signal 4–component 2 ($\zeta_{teor} = 15$e-3)				
CM	36 to −26.4	0.340-3.652	14.3e−3	−4.96
AM	36 to 3.36	0.340-2.072	14.9e-3	−0.44
PM	36 to 2.91	0.340-2.096	14.9e-3	−0.43

7. Experiment

The procedures were also tested on signals acquired from the lateral vibration of a uniform beam ($\rho = 7850\,\mathrm{kg/m^3}$, $E = 2.1 \times 10^5$ MPa), with the free-free boundary conditions. Fig. 7 shows the experimental set-up.

The list of accessories is:

B&K type 4384 accelerometer,
B&K Nexus conditioning amplifier, and
IBM-compatible personal computer with a 12-bit NI AT-MIO-16E-1 acquisition card.

Hysteretic damping was used as a model for the energy dissipation, according to Beards [23]

$$\zeta = \acute{\eta}/2, \tag{35}$$

where $\acute{\eta}$ is the hysteretic damping factor. Because the measured signal is asymptotic the measured acceleration is nearly proportional to the displacement (the error is negligible). Therefore, the acceleration data can be directly used for damping identification.

Fig. 8 shows the scalogram of the experimental data. The frequency (scale) range is from 200 to 2000 Hz. The first three natural frequencies can be clearly seen. To identify the damping ratio of the natural frequencies the following procedure is required:

- extract the *natural frequency* (can be done with a classical Fourier transform),
- extract the *ridge* (CM, AM or PM),
- extract the *skeleton*,
- calculate the envelope (Eq. (18)), and
- extract the damping ratio (Eq. (16)).

The CWT was calculated in the neighbourhood of each natural frequency, the maximum allowed deviation frequency was $\pm 0.5\%$ of the natural frequency and the frequency resolution of the CWT was about one-tenth of the maximum deviation frequency. The parameters of the CWT for each natural frequency are given in Table 6.

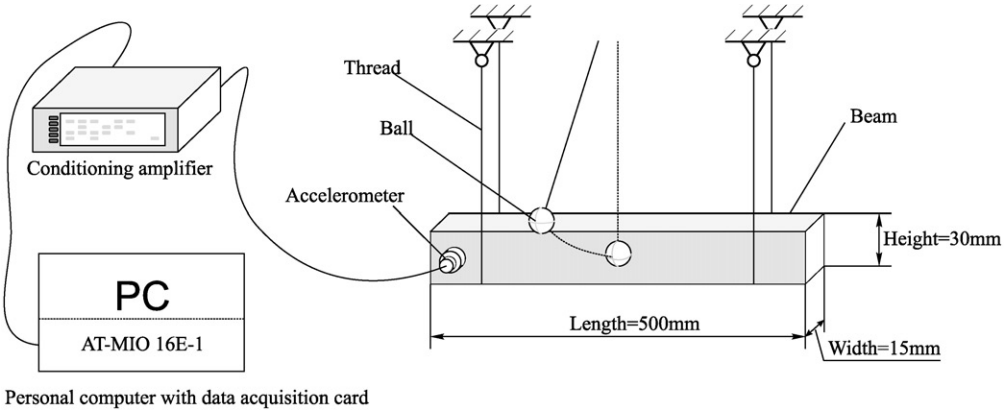

Fig. 7. Experiment set-up.

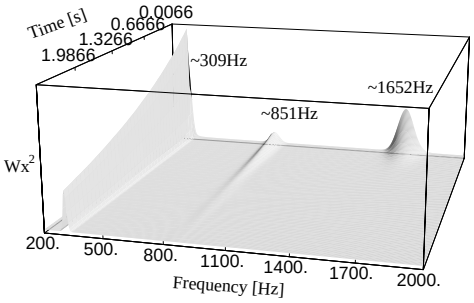

Fig. 8. Scalogram of the experimental data.

Table 6
Parameters of the CWT

Parameter	Natural frequency			Note
	1st	2nd	3rd	
Wavelet transform				
f_0 (Hz)≈	309	851	1652	Natural frequency
$\sigma_{1\ \mathrm{Hz}}$	3	5	6	Normalized σ
σ	99e-6	165e-6	198e-6	Parameter σ
Δf (Hz)	0.15	0.4	0.6	Frequency resolution
u_{wd} (ms)	25.06	15.19	9.38	Time-width
$\Delta\omega$ (Hz)	66	108	175	Band-width
η (Hz)		30303		Frequency modulation

The damping parameters for each natural frequency are given in Table 7. If the particular natural frequency is present for a relatively long time, then there is usually no need to use the identification procedures on the whole time-length. This was the case in the first two natural frequencies; the break point of damping identification is therefore not reached. However, by

Table 7
Damping identification on the beam

Method	Time-window (s)	ζ	$\eta = 2\zeta$
First natural frequency ($\approx$309 Hz)			
CM	0.025–4.924	120.6e–6	241.2e–6
AM	0.025–4.924	120.6e–6	241.2e–6
PM	0.025–4.924	120.6e–6	241.2e–6
Second natural frequency ($\approx$851 Hz)			
CM	0.015–3.284	164.3e–6	328.6e–6
AM	0.015–3.284	164.3e–6	328.6e–6
PM	0.015–3.284	164.3e–6	328.6e–6
Third natural frequency ($\approx$1652 Hz)			
CM	0.009–2.630	287.3e–6	574.6e–6
AM	0.009–1.152	391.2e–6	782.4e–6
PM	0.009–1.153	391.1e–6	782.2e–6

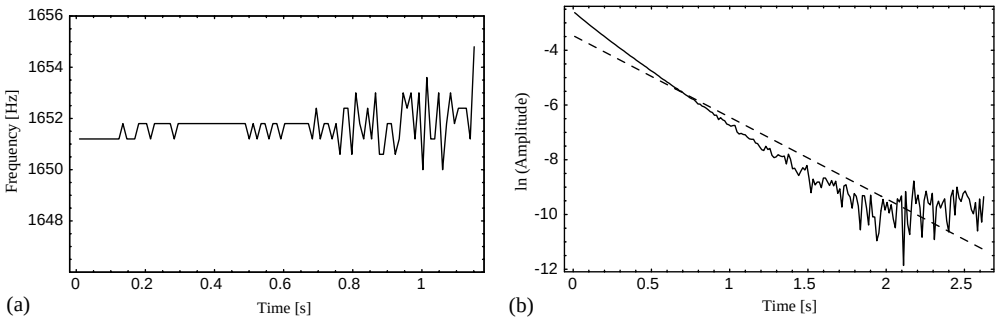

Fig. 9. (a) Ridge of third natural frequency of measured signal (using the PM); (b) logarithm of the amplitude of the third natural frequency (using the CM), —signal, - - - linear regression.

analyzing the damping at the third natural frequency, the AM reaches the break point at 1.152 s and the PM reaches it 1 ms later (Fig. 9a). As expected, the CM gives a wrong result (Fig. 9b).

According to Cremer et al. [24] the hysteretic damping parameter of the bending vibration of steel can be expected to be in the range from 200×10^{-6} to 600×10^{-6}. While the results for the tested, uniform beam are not so general, the hysteretic damping parameters given by Cremer should be understood as orientation values. However, the results seem to be in good agreement.

8. Conclusion

This study presents three methods for identifying damping: the cross-section method, the amplitude method and the phase method. The last two methods are especially appropriate because they provide feedback information about the noise, which can be used to stop the identification process. As is already known [19] for the ridge extraction the phase method was shown to be slightly better.

While other authors use the Morlet wavelet function, the Gabor wavelet function was used here. Consequently, the approximation of the continuous wavelet transform for the asymptotic signals was derived (Eq. (39)). The reason for choosing the Gabor wavelet function is the possibility of adapting its time and frequency spread.

This study also treats the instantaneous SNR, which provides a better description of the noise influence on the identification. It was found that the identification was still good, even with a noise of 0 dB, although for better results the noise should be less than 5 dB.

The analytically defined time length of the edge-effect is not only important for the case of automating the damping identification, but it is also important if the edge-effect needs to be reduced. The parameter σ of the Gabor wavelet has a critical influence on the edge-effect. A larger σ gives a lower frequency spread and is therefore more appropriate for analyzing close modes, a consequence of which is a slightly better resistance to noise. However, a larger σ also has some disadvantages: because the time spread increases the reconstruction gets worse; however, the time spread does not significantly affect the logarithm of the reconstructed envelope so the identification does not get worse. Usually, an appropriate parameter σ has to be chosen, on the one hand to ensure a small edge-effect and on the other hand, to have the opportunity to analyze close modes and to get a good reconstruction. By choosing a small parameter σ the shift of the amplitude extreme must be taken into account.

The procedures presented were also tested on a beam; the theoretical model of a damped model based on the hysteretic damping and the hysteretic damping factor was identified with the procedures. The results are in accordance with the literature [24].

Appendix A. Approximation of the continuous CWT of an asymptotic signal

According to Delprat [19] a sinusoidal signal, like those presented in Eq. (8), can be represented as a real part of an analytic signal $x(t) = \mathrm{Re}(x_a(t))$, where

$$x_a(t) = A(t)\,\mathrm{e}^{\mathrm{i}\,\varphi(t)}. \tag{A.1}$$

The connection between the CWT of an analytic and a real signal is $Wx(u,s) = \frac{1}{2}Wx_a(u,s)$ [14]. So the CWT of a real signal is

$$Wx(u,s) = \frac{1}{2}\int_{-\infty}^{+\infty} x(t)\,\psi^*_{Gabor_{u,s}}(t)\,\mathrm{d}t, \tag{A.2}$$

$$Wx(u,s) = \frac{1}{2}\int_{-\infty}^{+\infty} A(t)\,\mathrm{e}^{\mathrm{i}\varphi(t)}\frac{1}{\sqrt{s}}\frac{1}{(\sigma^2\pi)^{1/4}}\mathrm{e}^{-((t-u)/s)^2/(2\sigma^2)}\mathrm{e}^{-\mathrm{i}\eta(t-u)/s}\,\mathrm{d}t. \tag{A.3}$$

First substitute the time $t = t + u$, then use the Taylor power series expansion close to u: for the amplitude of order 0: $A(t+u) = A(u)$, and for the phase of order 1: $\varphi(t+u) = \varphi(u) + \varphi'(u)(t-u)$. After the integration the following expression is obtained:

$$Wx(u,s) = \tfrac{1}{2}A(u)\,\hat{\psi}_{Gabor_{u,s}}(\varphi'(u),\sigma,\eta)\,\mathrm{e}^{\mathrm{i}\,\varphi(u)} + Er\big(A'(t),\varphi''(u)\big). \tag{A.4}$$

Because of the Taylor expansion the generality is lost; however, if the frequency dissipation of the wavelet function is relatively small then the error $Er(A'(t),\varphi''(u))$ can be neglected (Eq. (11)) [14].

References

[1] W.T. Thomson, Theory of Vibration with Applications, 4th edition, Chapman & Hall, London, 1993.
[2] R.B. Randall, Vibration measurement equipment and signal analyzers, in: C.M. Harris (Ed.), Shock and Vibration Handbook, 3rd edition, McGraw-Hill, New York, 1987.
[3] A.D. Nashif, D.I.G. Jones, J.P. Henderson, Vibration Damping, 2nd edn, Wiley, New York, 1985.
[4] W.J. Staszewski, Identification of damping in mdof systems using time-scale decomposition, Journal of Sound and Vibration 203 (1997) 283–305.
[5] M. Boltežar, I. Simonovski, M. Furlan, Fault detection in DC electro motors using the continuous wavelet transform, *Meccanica*, in press.
[6] I. Simonovski, Valčna Analiza Nelinearnih Nestacionarnih Nihanj Elektromotorja, Wavelet Analysis of Nonlinear and Non-stationary Electro-motor Vibrations, Ph.D. Thesis, Slovene.
[7] I. Simonovski, M. Boltežar, Monitoring the instantaneous frequency content of a washing machine during startup, Strojniški vestnik–Journal of Mechanical Engineering 47 (2001) 28–44.
[8] P. Argoul, H.P. Yin, B. Guillermin, Use of the wavelet transform for the processing of mechanical signals, Proceedings of the 23rd ISMA Conference, Leuven, Vol. 1, Belgique, 1998, pp. 375–403.
[9] H.P. Yin, P. Argoul, Integral transforms and modal identification, Comptes Rendus Academie Sciences de Paris 327 (IIb) (1999) 777–783.
[10] C.H. Lamarque, S. Pernot, A. Cuer, Damping identification in multi-degree-of-freedom systems via a wavelet-logarithmic decrement—part 1: theory, Journal of Sound and Vibration 235 (2000) 361–374.
[11] S. Hans, E. Ibraim, S. Pernot, C. Boutin, C.H. Lamarque, Damping identification in multi-degree-of-freedom systems via a wavelet-logarithmic decrement—part 2: study of a civil engineering building, Journal of Sound and Vibration 235 (2000) 375–403.
[12] P. Argoul, S. Hans, F. Conti, C. Boutin, Time-frequency analysis of free oscillations of mechanical structures. Application to the identification of the mechanical behavior of buildings under shocks, in: J.A. Gemes (Ed.), COST F3 Conference: System Identification and Structural Health Monitoring, Universidad Politècnica de Madrid, Madrid, 2001, pp. 283–292.
[13] J. Slavič, Identifikacija Dušenja Nihajočih Sistemov z Več Prostostnimi Stopnjami z Uporabo Valčne Transformacije, Identification of Damping in Multi-degree-of-freedom Systems using Wavelet Transformation, Graduation Thesis, 2001, Slovene.
[14] S. Mallat, A Wavelet Tour of Signal Processing, 2nd edition, Academic Press, New York, 1999.
[15] C. Torrence, G.P. Compo, A practical guide to wavelet analysis, Bulletin of the America Meteorological Society 79 (1998) 61–78.
[16] A. Grossman, J. Morlet, Decomposition of hardy function into square integrable wavelets of constant shape, SIAM Journal of Mathematical Analysis and Applications 15 (1984) 723–736.
[17] P. Tchamitchian, B. Torresani, Ridge and skeleton extraction from the wavelet transform, in: M.B. Ruskai (Ed.), Wavelets and Their Applications, Jones and Bartlett, Boston, 1992, pp. 123–151.
[18] M. Ruzzene, A. Fasana, L. Garibaldi, B. Piombo, Natural frequencies and dampings identification using wavelet transform: Application to real data, Mechanical Systems and Signal Processing 11 (1997) 207–218.
[19] N. Delprat, B. Escudie, P. Guillemain, R.K. Martinet, Ph. Tchamitchian, B. Torresani, Asymptotic wavelet and Gabor analysis: extraction of instantaneous frequencies (special issue on Wavelet and Multiresolution Analysis), IEEE Transactions on Information Theory 38 (1992) 644–664.
[20] R.A. Carmona, W.L. Hwang, B. Torresani, Characterization of signals by the ridges of their wavelet transform, IEEE Transactions on Signal Processing 45 (1997) 2586–2590.
[21] K. Worden, Data processing and experiment design for the restoring force surface method, part 1: integration and differentiation of measured time data, Mechanical Systems, Signal Processing 4 (1990) 295–319.
[22] I. Grabec, J. Gradišek, Opis naključnih pojavov, Random data analysis, Fakulteta za strojništvo, Ljubljani, Slovene, 2000.
[23] C.F. Beards, Structural Vibration: Analysis and Damping, Arnold, Paris, 1996.
[24] L. Cremer, M. Heckl, Structure-Borne Sound, Springer, Berlin, 1973, pp. 205–217 (Chapter III).